RSC Advances

PAPER

Cite this: *RSC Adv.*, 2023, **13**, 30726

Molecular simulation of the rheological properties and shear thinning principles of supramolecular drilling fluids at different burial depths

Yunjie Li, *[ab] Qian Li,[a] Xiangyan Yang[c] and Mei Ning[d]

In order to investigate the rheological properties and shear thinning principles of supramolecular drilling fluids, the salt-responsive supramolecular ionomer polymers with different components were designed and the change in shear viscosity of supramolecular polymer drilling fluid system with shear rate was studied using the molecular dynamics simulation method. The result indicated that the ionic supramolecular polymer drilling fluid system exhibits better self-assembly performance than the nonionic acrylamide drilling fluid system. Moreover, the drilling fluid system exhibits the best rheological properties and self-assembly performance when the feeding ratios of the three monomers in the two polymers are $m:n:o = 5:90:5$ and $m:n:o = 30:40:30$, respectively. The shear viscosity recovery rate of the #3 ionic supramolecular polymer drilling fluid system at different burial depths (1–5 km) is >87%, where the shear viscosity is mainly determined at ambient pressure. The shear thinning phenomenon of the supramolecular polymer drilling fluid system occurs because of the combined effect of the polymer molecular orientation and entanglement structure. When the shear rate is above a critical value, the polymer molecules are oriented along the flow field direction, decreasing the shear viscosity. However, when the shear rate is very high, the entanglement structure of the molecules is opened and the mesh structure of the fluids is disrupted, decreasing the shear viscosity of the drilling fluid.

Received 26th July 2023
Accepted 2nd October 2023

DOI: 10.1039/d3ra05045a

rsc.li/rsc-advances

Introduction

Drilling fluids, also known as drilling hole flushing fluids, are the circulating flushing media used in drilling process, and they are the blood of well test, workover and drilling engineering.[1] The basic function of drilling fluid is to carry the broken rock debris to the surface *via* circulation, keep the hole clean, ensure contacts between the drill and bottom of the hole, and break the new formation.[2] When the circulation is stopped for some reason, the drilling cuttings can remain suspended in the well and are not sunken quickly by the drilling fluid, which can prevent the occurrence of settling sand or sticking.[3] In addition, it has the function of balancing and controlling the formation pressure, which can prevent blowout, leakage accidents, and formation pollution of drilling fluids.[4] The rheological property is a basic property of drilling fluids, which plays a very important role in solving the following aspects: carry cuttings and ensure that the bottom and hole are clean, make the cuttings suspended, improve the drilling rate, maintain borehole rules, and ensure downhole safety.[5,6] Not only is the stability of the viscosity of drilling fluids at different shear rates conducive to the borehole wall stability, but it can also ensure the stability of formation internal pressure, which is helpful to avoid accidents such as collapse and blowout during drilling.[7] The drilling fluids can be divided into water-based, oil-based, and gas-based drilling fluids, according to the dispersed medium (continuous phase), among which the water-based drilling fluids are the most environmentally friendly, economical and widely used drilling fluids.[8,9] At present, the rheological properties of water-based drilling fluids are generally unstable with changes in burial depth, temperature, shear rate, *etc.*, and those cannot be restored with the conditions changed, which becomes a potential safety hazard in the later construction process. Therefore, the development of new, efficient, and high-performance water-based drilling fluids is an effective way to reduce the cost and increase efficiency, and it has a wide application prospect.

There are many research reports on the modification of water-based drilling fluids by relevant technologies, mainly focusing on the polymer molecular modification of emulsion or the addition of nanomaterial additives to improve the performance of drilling fluids.[10,11] Razali *et al.* studied the effects of adding carbon nanomaterials on the rheology, emulsion

[a]*School of Oil and Gas Engineering, Southwest Petroleum University, Chengdu 610500, Sichuan Province, China. E-mail: yunjieli2016@sina.com*
[b]*Chongqing Branch of Daqing Oilfield Co., LTD, Chongqing 402660, China*
[c]*School of Foreign Languages, Chongqing Technology and Business University, Chongqing 400060, China*
[d]*The No. 1 Gas Production Plant, PetroChina Changqing Oilfield Company, Xi'an 710021, Shaanxi Province, China*

stability, and filtration control ability of ester-based drilling fluids.[12] Chu *et al.* introduced a series of amidocyanogen silanols (HASes) modified with methacryloxy propyl trimethoxyl silane (MPS) to improve the high-temperature-resistant shale inhibitors of water-based drilling fluids.[13] Li *et al.* designed new environmentally friendly water-based drilling fluids by adding LAPONITE® nanoparticles and polysaccharide/polypeptide derivatives.[14] In recent years, some scholars have proposed developing supramolecular drilling fluids with special rheological properties by supramolecular chemistry-related theories, which can significantly improve the shear dilution and pollution resistance of drilling fluids and the efficiency of injection drilling.[15,16] Supramolecular chemistry explores the interaction between two or more molecular chains *via* intermolecular forces to form supramolecular systems with specific structures and functions, including structures and functions of entities formed by the joining of two or more chemical species.[17,18] The mesh structure of the supramolecular drilling fluid treatment agent is disrupted at high shear rates, which reconnects into a three-dimensional spatial network structure at low shear rates.[19,20] The disruption is reversible, and the shear-damaged treatment agent reassembles when flowing through the annular space at low shear rates.[21,22] Therefore, an increased viscous shear and restored ability to carry rock chips and agglomerate materials allow for full jet drilling and increased drilling rates. Yang *et al.* synthesized a novel organic–inorganic polymer nanocomposite of LAPONITE® nanoparticles and polymers and studied its chemical structure and rheological properties.[23] Jiang *et al.* developed a supramolecular rheological modifier and a supramolecular filtrate reducer, and made the supramolecular drilling fluid system with these as the core. The results indicated that this drilling fluid system has better shear recovery and rheological properties closer to the ideal range than those of the conventional drilling fluids.[24] These research studies on the polymer molecular structure and rheological properties of supramolecular drilling fluid systems are experimental tests that obtain macroscopic conclusion, and they do not explain the essential mechanism and lack unified understanding and guidance.

In this work, the molecular dynamics simulation method was used to reveal the rheological properties of supramolecular drilling fluids at the molecular level. First, based on the designed ionic supramolecular polymer shear lifters and supramolecular filter loss reducers, a supramolecular drilling fluid system model with different molecular chain structures was established. Second, the molecular dynamics simulation method was used to study the change in the shear viscosity of the drilling fluid system at different shear rates and determine the ionic supramolecular polymer structure with the best rheological properties. Third, the variation law of the rheological properties of the supramolecular polymer drilling fluid system at different burial depths was simulated. Fourth, the main factors affecting the drilling fluid system were determined in terms of both ambient temperature and pressure. Finally, the shear thinning mechanism of the drilling fluid was theoretically investigated in terms of the supramolecular polymer orientation and molecular structure.

Model and calculation methods

Model construction

Simulations of supramolecular polymer solutions are rarely reported in the literature owing to the limited computational power and study scale. However, some researchers have performed and reported simulation studies on the properties of polymer solutions, which provide a basis for this study. In this work, polyacrylamides, the most widely studied polymers, were used as the object of study for supramolecular polymer drilling fluids. Supramolecular polymers were formed by the copolymerization of nonionic monomer acrylamide (AM), anionic monomer 2-acrylamido-2-methylpropane sulfonic acid (AMPS), and cationic monomer (3-acrylamidopropyl)trimethylammonium chloride (TAC). The molecular structures of the monomers of the supramolecular polymer are shown in Fig. 1.

Salt-responsive supramolecular ionomers were formed by copolymerization of AM, AMPS, and TAC. The simplified formula of the molecular structure is noted as (PMPS)*m*–(PAM)*n*–(PTAC)*o*, as shown in Fig. 2. The supramolecular ionomer polymers contain two types of polymers, namely, high-molecular-weight low-ionic-concentration (HvL) and low-molecular-weight high-ionic-concentration (LvH) polymers. HvL and LvH polymers were obtained by adjusting the molar feeding ratio of the three monomers, namely, AM, AMPS, and TAC. To determine the optimal feeding ratio of the three monomers in HvL and LvH polymers, the proportioning parameters for the designed supramolecular polymer monomers were specified (Table 1). Additionally, nonionic monomer AM-based supramolecular polymer was set as 1#, as a comparison group.

The main components of the supramolecular drilling fluid system formulation were designed based on the studies by Jiang *et al.* and Vryzas *et al.*[25,26] (Table 2). The components that did not affect the drilling fluid performance were removed to simplify the drilling fluid model. Additionally, bentonite, a supramolecular polymer, an inert plugging agent, NaCl, and barite were selected as the components of the supramolecular drilling fluid in the model.

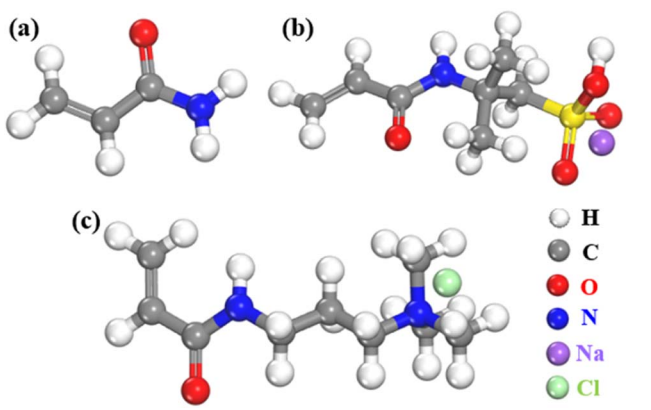

Fig. 1 Molecular structures of supramolecular ionomer monomers: (a) AM, (b) AMPS, and (c) TAC.

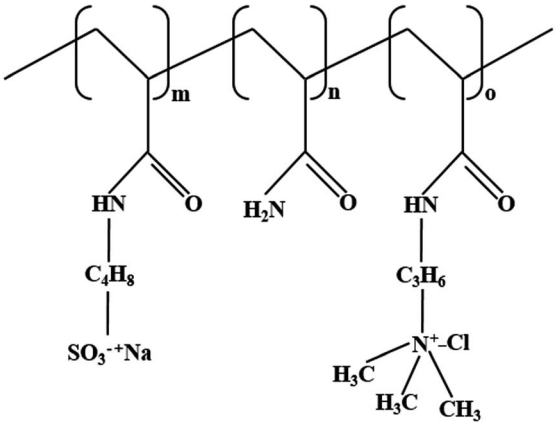

Fig. 2 Simplified molecular formula of the salt-responsive supramolecular ionomer.

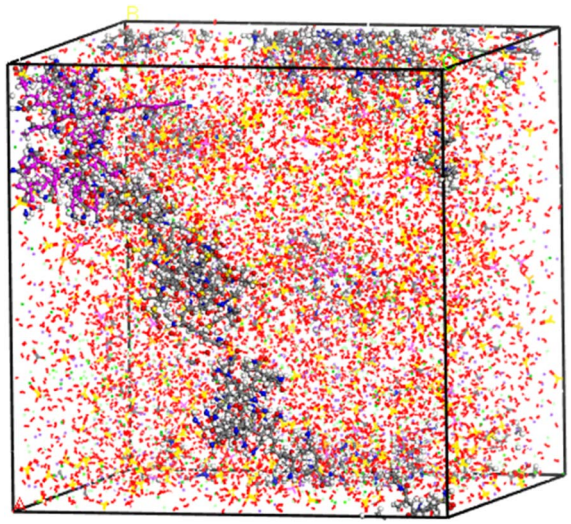

Fig. 3 Supramolecular polymer drilling fluid model.

Table 1 Monomer parameters of the salt-responsive supramolecular ionomer

Number	HvL	LvH
1#	$(PMPS)_0$–$(PAM)_{100}$–$(PTAC)_0$	$(PMPS)_0$–$(PAM)_{100}$–$(PTAC)_0$
2#	$(PMPS)_3$–$(PAM)_{94}$–$(PTAC)_3$	$(PMPS)_{35}$–$(PAM)_{30}$–$(PTAC)_{35}$
3#	$(PMPS)_5$–$(PAM)_{90}$–$(PTAC)_5$	$(PMPS)_{30}$–$(PAM)_{40}$–$(PTAC)_{30}$
4#	$(PMPS)_7$–$(PAM)_{86}$–$(PTAC)_7$	$(PMPS)_{25}$–$(PAM)_{50}$–$(PTAC)_{25}$

The model of supramolecular drilling fluid was built using the Materials Studio 2019 software. Take the 3# supramolecular drilling fluid, for example; first, we opened seven 3D atomistic pages of the visualizer module and built the models of $(PMPS)_5$–$(PAM)_{90}$–$(PTAC)_5$, $(PMPS)_{30}$–$(PAM)_{40}$–$(PTAC)_{30}$, bentonite, NaCl, H_2O, sealers and barite, in turn. Second, we opened the calculation function of Amorphous Cell module and imported the above-mentioned seven molecular models. Third, we set the number of molecular models to 1, 1, 50, 1200, 5200, 157 and 515, respectively. Finally, we clicked the run button to start the modelling process. The size of the supramolecular drilling fluid model is 66.68 nm × 66.68 nm × 66.68 nm and the corresponding density is 1.8 g cm^{-3}, as shown in Fig. 3.

Research methods

All calculations were performed using the Amorphous Cell and Forcite modules of Materials Studio 2019 developed by Accelrys Inc. Atomic interactions were performed using the condensed-phase optimized molecular potentials for atomistic simulation studies (COMPASS) force field, which has been recently developed and is suitable for oil–water two-phase flow simulations. The simulations were performed with three aspects: geometry optimization, kinetic relaxation, and nonequilibrium molecular dynamics simulations.

Geometry optimization includes geometry optimization of the supramolecular drilling fluid model structure to reduce or eliminate geometrical irrational factors such as molecular overlap during the model construction process and obtain the lowest energy state or conformation of the system. Smart Algorithm was chosen as the geometry optimization algorithm, wherein COMPASS was used as the potential energy model and the molecular charge distribution model was Forcefield assigned. Additionally, a group-based summation method was used to calculate the electrostatic and van der Waals forces.

Kinetic relaxation is an equilibrium molecular dynamics simulation process that takes into account the thermal motion of molecules, so that they reach the most stable state during the dynamic motion, that is, kinetic relaxation, is used to find the lowest energy state of the dynamic process. COMPASS was chosen as the potential energy model. The NPT constant-temperature and constant-pressure ensemble was chosen as the ensemble used in this study. The velocity distribution model followed a random distribution satisfying the Maxwell–Boltzmann distribution law, where the simulated temperatures were 310 K, 340 K, 370 K, 400 K, and 430 K and the corresponding pressures were 15 MPa, 30 MPa, 45 MPa, 60 MPa, and 75 MPa, respectively. Additionally, the simulation time step was 1 fs, and the total simulation time was 1000 ps. One frame was output every 1000 steps, and a total of 1000 frames could be output. The Nosé–Hoover–Langevin method (Q ratio = 0.01, decay constant = 0.1 ps) was used to control the temperature. The selected charge model was Forcefield assigned. Moreover, the

Table 2 Formulation of the supramolecular drilling fluid system (mass fraction/%)

Bentonite	Supramolecular polymer	Inert plugging agent	NaCl	Barite	Solvent	pH	Tackifier	Coating agent
3.5	6.0	7.0	35.0	Adjust system density to 1.8 g cm^{-3}	46.0	0.5	1.0	1.0

summation of electrostatic and van der Waals was performed using the group-based summation method.

Nonequilibrium molecular dynamics simulations were performed to calculate the shear viscosity of supramolecular drilling fluids. First, on the basis of the optimized model obtained in the previous two steps, the confined shear calculation function of the Forcite module was opened. Second, the relevant calculation parameters were set as follows: the COMPASS was chosen as the Forcefield, along with the NPT constant-temperature and constant-pressure ensemble. The simulated temperatures were set to 310 K, 340 K, 370 K, 400 K, and 430 K, and the corresponding pressures were 15 MPa, 30 MPa, 45 MPa, 60 MPa, and 75 MPa, respectively. Third, to investigate the self-assembling properties of the supramolecular polymer drilling fluid system when the shear rate changed from high to low, the shear rate was further reduced to calculate the corresponding shear viscosity using the simulation model of the increasing shear rate process. Therefore, the shear rate ranged from 1.0×10^{-4} ps^{-1} to 1.0 ps^{-1} to 1.0×10^{-4} ps^{-1} and the simulation time was 1000 ps. The temperature and pressure of the drilling fluid system were controlled using the Nosé–Hoover–Langevin and Berendsen methods, respectively, where the charge mode was set to Forcefield assigned. Electrostatic forces and van der Waals forces were calculated using the group-based summation method. Shear periodic boundary conditions were chosen for simulations.

Results and discussion

Shear characteristics of different drilling fluid systems

The shear viscosity of the drilling fluid as it flows through the nanopore space can be calculated using eqn (1):

$$\eta = \tau_{xy}/\dot{\gamma} \quad (1)$$

where τ_{xy} is the shear stress applied to the drilling fluid and $\dot{\gamma}$ is the shear rate. According to eqn (1), the instantaneous shear viscosity of the drilling fluid was calculated at 1 ps intervals. Subsequently, the change in shear viscosity with time was determined based on the cumulative averaging method.

To study the shear thinning characteristics of salt-responsive supramolecular polymer drilling fluids, drilling fluid systems with different types of supramolecular polymer chain structures were designed. The simulation process was divided into three stages, in which the shear rate increased (stage 1), reached equilibrium (stage 2) and decreased (stage 3). Stage 1 and stage 3 represent the shearing and self-assembly processes of the drilling fluid system, respectively. Additionally, the rheological curves at different shear rates were calculated (Fig. 4). Except for the position between 2.5×10^{-3} ps^{-1} and 5.0×10^{-4} ps^{-1} in the shear rate increase phase, the viscosity of the ionic supramolecular polymer drilling fluid system with different ratios at different shear rates was higher than that of the nonionic AM supramolecular polymer drilling fluid, indicating the better rheological properties and self-assembly performance of the ionic supramolecular polymer drilling fluid. Throughout the simulation, the rheological curves showed three stages:

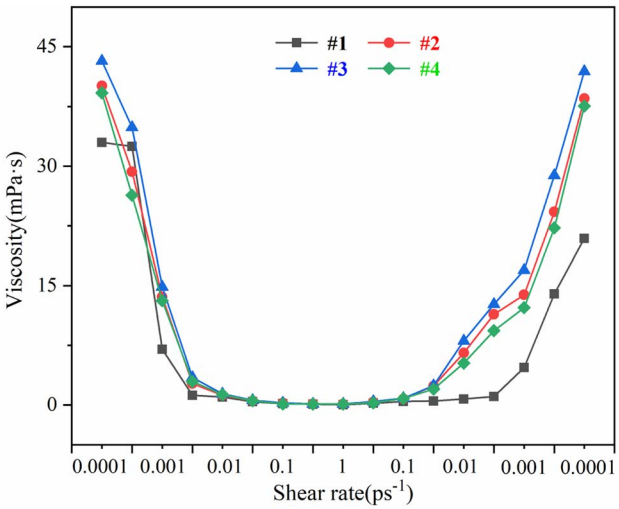

Fig. 4 Rheology curves of different drilling fluid systems.

decreasing, equilibrium, and increasing. When the shear rate increases from 1.0×10^{-4} ps^{-1} to 1.0 ps^{-1}, the shear viscosity of the drilling fluid decreases rapidly when $\dot{\gamma} < 1.0 \times 10^{-2}$ ps^{-1}, leading to shear thinning. When $\dot{\gamma} > 1.0 \times 10^{-2}$ ps^{-1}, the shear viscosity of the drilling fluid remains basically unchanged. When the shear rate decreases from 1.0 ps^{-1} to 1.0×10^{-4} ps^{-1} and $\dot{\gamma} < 1.0 \times 10^{-1}$ ps^{-1}, the shear viscosity of the drilling fluid decreases and the value remains basically unchanged. When $\dot{\gamma} > 1.0 \times 10^{-1}$ ps^{-1}, the shear viscosity of the drilling fluid gradually increases with the decrease in shear rate. When $\dot{\gamma} > 1.0 \times 10^{-3}$ ps^{-1}, the shear viscosity rapidly increases. Due to the partial bond breaking of pure PAM polymer chains at a high shear rate that this failure is irreversible, it is difficult for the viscosity to recover to the original level during the reduction of shear rate. For the supramolecular ionic polymer chain after the structure is destroyed at a high shear rate, the three-dimensional spatial network structure will be reassembled and the viscosity can be increased to more than 87% of the original at low shear state stage. At this time, the shear viscosity of the ionic supramolecular polymer drilling fluid system is significantly higher than that of the nonionic AM supramolecular polymer drilling fluid. Therefore, the ionic supramolecular polymer drilling fluid system exhibits a better self-assembling performance than that of the nonionic AM supramolecular polymer drilling fluid when the shear rate decreases from the maximum. Additionally, the ionic supramolecular polymer drilling fluid system can rapidly restore the morphology of the polymer molecular chains, resulting in more pronounced salt responsiveness. Compared with the #2 and #4 drilling fluid systems, the #3 ionic supramolecular polymer drilling fluid system has the highest shear viscosity in the increasing and decreasing shear rate phases. Therefore, when the polymerization degrees of the three monomers (AM, AMPS, and TAC) in the two polymers (HvL and LvH) were $m : n : o = 5 : 90 : 5$ and $m : n : o = 30 : 40 : 30$, respectively, the drilling fluid system exhibited relatively best rheological properties and self-assembly performance, which is consistent with the research result of Arain *et al.*[27]

Variation in the rheological properties of the drilling fluid at different burial depths

To study the rheological properties of supramolecular drilling fluids at different burial depths, temperature and pressure gradients of 30 K km^{-1} and 15 MPa km^{-1} in a reservoir environment were used. Herein, the burial depths of drilling fluids ranged from 1 to 5 km. The simulated temperature and pressure parameters at different burial depths are shown in Table 3.

According to the conclusion in the previous section, the #3 ionic supramolecular drilling fluid system exhibits the best rheological performance. Therefore, this system was used for subsequent simulations. The change in the rheological properties of the supramolecular polymer drilling fluid system with the shear rate at different burial depths is shown in Fig. 5. At different burial depths, the supramolecular polymer drilling fluid system showed a decreasing (<1.0 × 10^{-2} ps^{-1})-equilibrium (1.0 × 10^{-2} ps^{-1} to 1.0 ps^{-1} to 1 × 10^{-2} ps^{-1})-increasing (>1 × 10^{-2} ps^{-1}) trend with the change in shear rate. Therefore, this supramolecular polymer drilling fluid system also exhibits self-assembly properties at geological burial depths. As the shear rate decreases from the maximum value, the shear viscosity of the drilling fluid increases. Additionally, it was observed that the viscosity of the drilling fluid increases and decreases, exhibiting regular changes (increase or decrease) in drilling fluid viscosity with repeatedly varying high and low shear rate conditions. A comparison of the shear viscosity at the initial and final shear rates of 1 × 10^{-4} ps^{-1} at different burial depths shows that the shear viscosity recovery rate of the ionic supramolecular polymer drilling fluid system is >87%. At high shear rates, the polymer molecular chains of this drilling fluid system are disrupted. At lower shear rates, the polymer molecular chain of this drilling fluid system reassembles to restore the shear viscosity of the drilling fluid. The different burial depths are mainly determined by a combination of environmental parameters, temperature, and pressure. To determine the most important influencing parameters, temperature and pressure were studied separately.

The rheological curves of the #3 drilling fluid system at 298 K, 310 K, 340 K, 370 K, 400 K, and 430 K are shown in Fig. 6, where the ambient pressure is 5 MPa. The shear viscosity of the

Table 3 Environmental parameters of shale reservoirs at different burial depths

Burial depth (km)	Temperature (K)	Pressure (MPa)
1	310	15
2	340	30
3	370	45
4	400	60
5	430	75

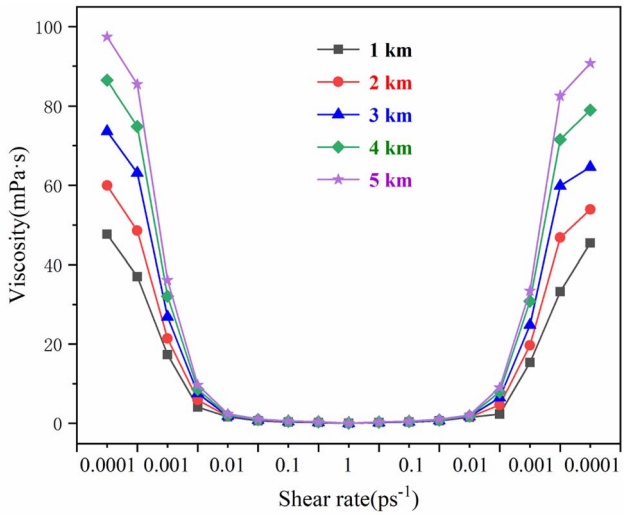

Fig. 5 Rheology curves of the #3 drilling fluid system at different burial depths.

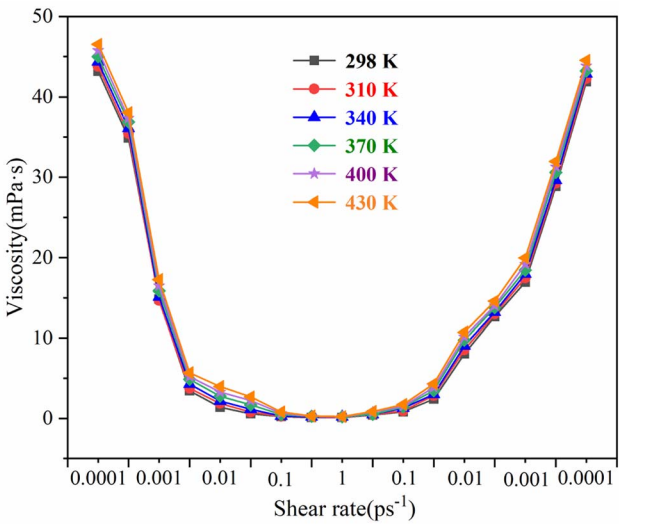

Fig. 6 Rheology curves of the #3 drilling fluid system at different temperatures.

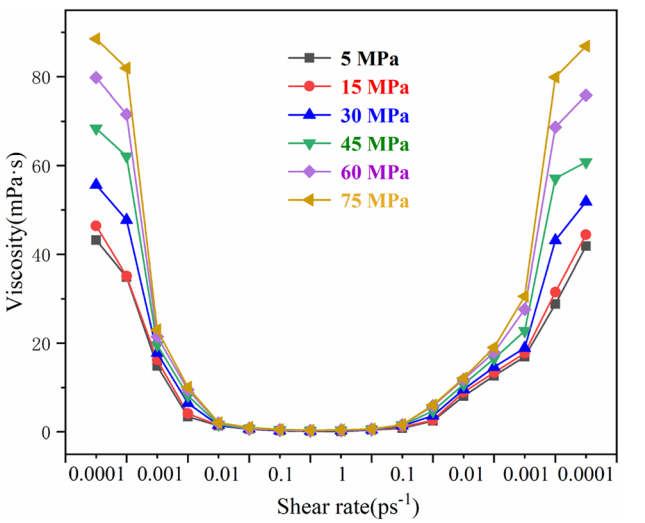

Fig. 7 Rheology curves of the #3 drilling fluid system at different pressures.

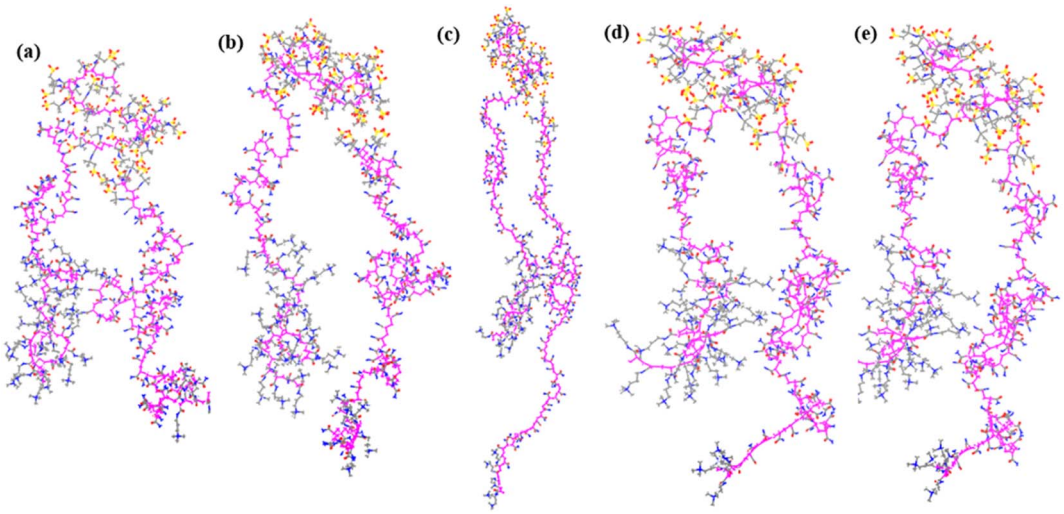

Fig. 8 Orientation distribution of supramolecular polymers at shear rates of (a) 1.0×10^{-4} ps^{-1}, (b) 1.0×10^{-3} ps^{-1}, (c) 1.0×10^{-2} ps^{-1}, (d) 1.0×10^{-1} ps^{-1}, and (e) 1.0 ps^{-1} at 430 K.

drilling fluid system increases with the increase in ambient temperature. Overall, the temperature has a small effect on the rheological properties of the drilling fluid system. The corresponding shear viscosity of the drilling fluid is <1 mPa s for every 30 K increase in the ambient temperature.

The rheological curves of the 3# drilling fluid system at 5 MPa, 15 MPa, 30 MPa, 45 MPa, 60 MPa, and 75 MPa are shown in Fig. 7, where the ambient temperature is 298 K. The shear viscosity of the drilling fluid system increases with the increase in ambient pressure. The effect of pressure on the shear viscosity of the drilling fluid is most obvious in the low-shear range at the shear thinning stage and the self-assembly process, where a higher pressure leads to a more pronounced increase in shear viscosity.

Shear thinning mechanism of the drilling fluid

The change in the viscosity of salt-responsive supramolecular polymer drilling fluids with shear rates is usually related to the orientation of fluid molecules in the drilling fluid along the flow field and the entanglement structure of supramolecular polymers. A slice of the simulated box was intercepted to study the orientation of the supramolecular polymer with the shear flow field. Only the carbon chains of two supramolecular polymers, $m:n:o = 5:90:5$ and $m:n:o = 30:40:30$, were retained to obtain clearer results. The orientation distribution of the supramolecular polymers at different shear rates at a simulated temperature of 430 K and a pressure of 75 MPa was observed (Fig. 8a–e). The orientation of the supramolecular polymers gradually increases as the shear rate increases. When the shear rate is very large (Fig. 8d and e), the molecular orientation no longer increases with the shear rate, consistent with the related literature. Tucker *et al.* simulated the change in the orientation of the measured fibers in the shear and tensile flow fields with the strength of the flow field.[28] Their results indicate that molecules are oriented along the direction of the flow field as the shear rate increases. However, when the shear rate exceeds a critical value, the ordering reaches a limit and no longer increases, in agreement with experimental observations. Moor *et al.* studied the rheological behavior of $C_{100}H_2O_2$ under shear and concluded that at low shear rates, the orientation angles of the molecular chains are clearly induced by shear; therefore, the molecules exhibit an ordered arrangement.[29] At high shear rates, the orientation angles of the molecules approach the limiting values and no longer change with the shear rate.

When a supramolecular polymer flows under the action of a shear flow field, there is a velocity gradient between the layers. In different flow layers, long-chain molecules can lead to stretching deformation due to the different flow velocities in each layer, which increases their stress. Additionally, the molecules adjust their conformation at any time using thermal motion, so they are in the same flow layer as much as possible and relax the externally applied stress. Therefore, the polymer molecules show a directional arrangement with the shear flow field. As the molecules are arranged in the shear direction, the increased fluidity of the drilling fluid decreases the corresponding viscosity, producing the effect of polymer molecular orientation on the viscosity of the drilling fluid.

Conclusions

The viscosity of a drilling fluid is an important factor that determines its rheological properties. However, the shear rate also has an important effect on the rheological properties of the drilling fluid. In this work, different types of drilling fluid systems were established using the molecular dynamics simulation method with an ionic supramolecular polymer as the object. Additionally, the rheological behavior at different shear rates was studied. Subsequently, the mechanism of the change in the viscosity with shear rates was explained from a microscopic perspective. The conclusions of this study are as follows:

(1) Except for the position between 2.5×10^{-3} ps^{-1} and 5.0×10^{-4} ps^{-1} in the shear rate increase phase, the viscosities of the

ionic supramolecular polymer drilling fluid systems with different ratios were greater than those of the nonionic AM supramolecular polymer drilling fluid systems, indicating that the ionic supramolecular polymer drilling fluid exhibits better rheological properties and self-assembly performance. The drilling fluid systems exhibit relatively best rheological properties and self-assembly performance when the feeding ratios of three monomers, namely, AM, AMPS, and TAC in two polymers, namely, HvL and LvH are $m:n:o = 5:90:5$ and $m:n:o = 30:40:30$, respectively.

(2) The supramolecular polymer drilling fluid system self-assembles at the geological burial depth, and its shear viscosity recovery rate is >87%. When the shear rate decreases from the maximum value, the shear viscosity of the drilling fluid increases, exhibiting regular changes (increase or decrease) in drilling fluid viscosity with repeatedly varying high and low shear rate conditions. The ambient temperature of the burial depth has little influence on the rheological performance of the supramolecular drilling fluid, and the ambient pressure is the main factor that determines the rheological performance of the supramolecular drilling fluid.

(3) The shear thinning phenomenon of ionic supramolecular polymers results from the combined effect of the molecular orientation and entanglement structure. When the shear rate exceeds a critical value, the polymer molecules are oriented along the direction of the flow field, decreasing the fluid flow resistance and shear viscosity. When the shear rate is very high, the entanglement structure of the molecules is open. Accordingly, the disrupted fluid web structure decreases the viscosity of the drilling fluid.

Author contributions

Yunjie Li: conceptualization, methodology, data curation, writing-original draft, supervision. Qian Li: guidance, investigation. Xiangyan Yang: test data comparison, rationality analysis. Mei Ning: software, visualization, model optimization.

Conflicts of interest

There are no conflicts to declare.

Acknowledgements

The authors would like to acknowledge support from the National Key R&D Projects (2019YFA0708303), the Science and Technology Cooperation Project of the CNPC-SWPU Innovation Alliance (2020CX040102, 2020CX040201).

References

1 A. Ahmed, S. Elkatatny and S. A. Onaizi, *Geotech. Geol. Eng.*, 2023, **229**, 212137.
2 J.-S. Sun, Z.-L. Wang, J.-P. Liu, K.-H. Lyu, X.-B. Huang, X.-F. Zhang, Z.-H. Shao and N. Huang, *Petrol. Explor. Dev.*, 2022, **49**, 1161–1168.
3 J.-S. Sun, X.-F. Chang, K.-L. Lv, J.-T. Wang, F. Zhang, J.-F. Jin, X.-Y. Zhou and Z.-W. Dai, *Colloids Surf., A*, 2021, **621**, 126482.
4 G.-C. Jiang, T.-F. Dong, K.-X. Cui, Y.-B. He, X.-H. Quan, L.-L. Yang and Y. Fu, *Petrol. Explor. Dev.*, 2022, **49**(3), 577–585.
5 S. Moradi, A. Nowroozi and M. Shahlaei, *RSC Adv.*, 2019, **9**, 4644–4658.
6 B. Chen, C. Li, C.-J. Zhang, Y. Huang, G. Liu, D. Yan and M.-B. Xu, *Science Technology and Engineering*, 2022, **22**(4), 1408–1415.
7 T. Chen, N. Zhang, S.-C. Yang, J.-T. Cai, M. Li and N. Pokawin, *Appl. Chem. Ind.*, 2021, **50**(7), 1998–2007.
8 Y.-S. Zheng, Z.-H. Zhuo, Q. Mo and J.-S. Li, *Prog. Chem.*, 2011, **23**(9), 1862–1870.
9 B.-Q. Xie, A. P. Tchameni, M.-W. Luo and J.-T. Wen, *Mater. Lett.*, 2021, **284**, 128914.
10 X.-Y. Zhao, D.-Q. Li, H.-M. Zhu, J.-Y. Ma and Y.-X. An, *RSC Adv.*, 2022, **12**, 22853–22868.
11 L. Pu, P. Xu, M.-B. Xu, J.-J. Song, M. He and M.-D. Wei, *J. Petrol. Sci. Eng.*, 2022, **219**, 111053.
12 S. Z. Razali, R. Y. Yunus, D. Kania, S. A. Rashid, L. H. Ngee, G. Abdulkareem-Alsultan and B. M. Jan, *J. Mater. Res. Technol.*, 2022, **21**, 2891–2905.
13 Q. Chu, J.-L. Su and L. Lin, *Appl. Clay Sci.*, 2020, **185**, 105315.
14 X.-L. Li, G.-C. Jiang, Y. Xu, Z.-Q. Deng and K. Wang, *Petrol. Sci.*, 2022, **19**, 2959–2968.
15 K. S. Mali, N. Pearce, S. D. Feyter and N. R. Champness, *Chem. Soc. Rev.*, 2017, **46**, 2520–2542.
16 G. Bruce, J. Tony and S. Jonathan, *Chem. Commun.*, 2020, **56**, 6467–6468.
17 K. Ollerton, R.-L. Greenaway and A.-G. Slater, *Front. Chem.*, 2021, **9**, 774987.
18 S. B. Khan and S. L. Lee, *Molecules*, 2021, **26**, 3995.
19 T. A. Ali, *Nat. Rev. Chem.*, 2021, **5**, 442–443.
20 Y.-Y. Liu, P. K. Chen, J. H. Luo, G. Zhou and B. Jiang, *Acta Phys.-Chim. Sin.*, 2010, **26**(11), 2907–2914.
21 R. E. Swai, *J. Pet. Explor. Prod. Technol.*, 2020, **10**, 3515–3532.
22 J. Feng, J. Fu, P. Chen, Z. Du and L. Qing, *J. Nat. Gas Sci. Eng.*, 2016, **36**, 424–433.
23 J. Yang, J.-S. Sun, R. Wang, F. Liu, J.-T. Wang, Y.-Z. Qu, P.-Q. Wang, H.-J. Huang, L.-M. Liu and Z.-L. Zhao, *Colloids Surf., A*, 2022, **655**, 130261.
24 G.-C. Jiang, T.-F. Dong, K.-X. Cui, Y.-B. He, X.-H. Quan, L.-L. Yang and Y. Fu, *Petrol. Explor. Dev.*, 2022, **49**(3), 577–585.
25 G.-C. Jiang, Y.-B. He, W.-G. Cui, L.-L. Yang and C.-X. Ye, *Petrol. Explor. Dev.*, 2019, **46**(2), 385–390.
26 Z. Vryzas, V. C. Kelessidis, L. Nalbantian, V. Zaspalis, D. I. Gerogiorgis and Y.-M. Wubulikasimu, *Appl. Clay Sci.*, 2017, **136**, 26–36.
27 A. H. Arain, S. Ridha, R. R. Suppiah, S. Irawan and S. U. Ilyas, *J. Petrol. Sci. Eng.*, 2022, **219**, 111141.
28 J. Wang, J. F. O'Gara and C. L. Tucker, *J. Rheol.*, 2008, **52**, 1179–1200.
29 J. D. Moor, S. T. Cui, H. D. Cochran and P. T. Cummings, *J. Non-Newtonian Fluid Mech.*, 2000, **93**, 83–99.